University of Groningen

Variation in Flame Temperature with Burner Stabilization in 1D Premixed Dimethyl Ether/Air Flames Measured by Spontaneous Raman Scattering

Dai, Liming; Mokhov, Anatoli; Levinsky, Howard

Published in:
Energy & fuels

DOI:
10.1021/acs.energyfuels.9b03097

IMPORTANT NOTE: You are advised to consult the publisher's version (publisher's PDF) if you wish to cite from it. Please check the document version below.

Document Version
Publisher's PDF, also known as Version of record

Publication date:
2019

Link to publication in University of Groningen/UMCG research database

Citation for published version (APA):
Dai, L., Mokhov, A., & Levinsky, H. (2019). Variation in Flame Temperature with Burner Stabilization in 1D Premixed Dimethyl Ether/Air Flames Measured by Spontaneous Raman Scattering. *Energy & fuels*, *33*(11), 11976-11984. https://doi.org/10.1021/acs.energyfuels.9b03097

Copyright
Other than for strictly personal use, it is not permitted to download or to forward/distribute the text or part of it without the consent of the author(s) and/or copyright holder(s), unless the work is under an open content license (like Creative Commons).

The publication may also be distributed here under the terms of Article 25fa of the Dutch Copyright Act, indicated by the “Taverne” license. More information can be found on the University of Groningen website: https://www.rug.nl/library/open-access/self-archiving-pure/taverne-amendment.

Take-down policy
If you believe that this document breaches copyright please contact us providing details, and we will remove access to the work immediately and investigate your claim.

Downloaded from the University of Groningen/UMCG research database (Pure): http://www.rug.nl/research/portal. For technical reasons the number of authors shown on this cover page is limited to 10 maximum.

This is an open access article published under a Creative Commons Non-Commercial No Derivative Works (CC-BY-NC-ND) Attribution License, which permits copying and redistribution of the article, and creation of adaptations, all for non-commercial purposes.

energy&fuels

Article

Cite This: Energy Fuels 2019, 33, 11976−11984

pubs.acs.org/EF

Variation in Flame Temperature with Burner Stabilization in 1D Premixed Dimethyl Ether/Air Flames Measured by Spontaneous Raman Scattering

Liming Dai, Anatoli Mokhov,* and Howard Levinsky

Energy and Sustainability Research Institute Groningen, University of Groningen, 9747AG Groningen, The Netherlands

ABSTRACT: The flame temperatures in flat, laminar premixed dimethyl ether (DME)/air flames with varying degrees of burner stabilization were measured by spontaneous Raman scattering in a range of equivalence ratio (φ) from 0.6 to 2.0. Three commonly used mechanisms to describe DME oxidation were evaluated by comparing the calculated variation of flame temperature derived from one-dimensional flame calculations as a function of DME/air exit velocity with those obtained from the measurements. The results showed the necessity of incorporating radiative heat losses in the flame calculations. The three mechanisms yield similar results at φ = 0.6 and 2.0, underpredicting the temperatures more than 30 K. Differences between the measured and predicted temperatures for burner-stabilized flames are seen to indicate whether a free-flame burning velocity (S_L) is too high or too low. The results suggest a free-flame burning velocity of ∼14 cm/s at φ = 0.6, 2 cm/s lower than the mechanisms predicted, and burning velocities closer to 49 and 40 cm/s for φ = 1.0 and 1.4, respectively. Sensitivity analysis of the DME/air flame temperature as a function of exit velocity shows that the DME decomposition reaction and H abstraction from DME become important in the rich flames at φ = 1.7 and 2.0.

Downloaded via UNIV GRONINGEN on December 19, 2019 at 09:53:23 (UTC).
See https://pubs.acs.org/sharingguidelines for options on how to legitimately share published articles.

1. INTRODUCTION

With increasingly stringent emission regulations for internal combustion engines and the desire to replace fossil fuels, dimethyl ether (CH_3OCH_3, DME) has significant advantages as a future fuel. First, it has a high cetane number, making DME a candidate for use in diesel engines. Second, DME has no C−C bonds, decreasing the tendency of soot formation.[1] Moreover, it has a vapor pressure similar to that of LPG, and hence can be used in the existing infrastructures for transportation and storage.[2] Additionally, it has been reported that emissions of soot, nitrogen oxides, carbon monoxide, and unburned hydrocarbon are indeed lower in DME-fueled engines when using exhaust gas recirculation and proper injection strategies.[1,3−5] Well-tested DME chemical mechanisms would support the design and optimization of new engines specifically intended for DME as a fuel. However, compared with hydrogen, or even methane, the oxidation mechanism for DME is complex and contains more species and reactions with larger uncertainties in reaction rates. Thus, the performance of a DME mechanism requires experimental verification over as wide a range of flame parameters as possible. Premixed laminar flame studies play an important role in testing chemical mechanisms since they provide data, such as burning velocities and species profiles, amenable to experimental investigation under well-defined conditions, which can be used to compare with the predictions of numerical simulations. The majority of the experimental flame studies performed to date report the determination of free-burning velocities.[6−8] However, only the equivalence ratio, pressure, and temperature of the unburned gas can be varied in this kind of experiment, where temperature variation is performed by heating the unburned air−gas mixture.[9] We are not aware of previous studies examining flame conditions in which the burning velocity is below that of the free-flame, having flame temperatures below the adiabatic value. These conditions can be achieved in burner-stabilized flames, where heat transfer to the burner reduces the burning velocity to the exit velocity. To a certain extent, this is equivalent to decreasing the temperature of the unburned air−gas mixture.[10]

In this paper, we employ a method for exploring nonadiabatic conditions for testing the performance of chemical mechanisms for DME oxidation with respect to the burning velocity.[11] To be specific, we use the method proposed by Kaskan[12] to change the flame temperature by varying the exit velocity of the unburned air/fuel mixture in a one-dimensional (1D) burner. The flame temperature is measured as a function of exit velocity for DME/air mixtures and then compared with the temperatures obtained from 1D flame calculations. Here, the flame temperature is measured using spontaneous Raman scattering. As will be shown below, this method can produce data with an accuracy of ∼30 K.

2. EXPERIMENTAL SETUP AND MODELING

2.1. Burner System. Dimethyl ether with a purity of 99.8% was used as fuel. Flames at different equivalence ratios (φ) and flow rates were stabilized on a 6 cm diameter McKenna water-cooled bronze burner using the same setup as reported previously,[11] including the use of the nitrogen shroud. The equivalence ratios and exit velocities (v) of the unburned mixtures at room temperature were derived from the mass flow rates of fuels and air, which were measured by calibrated Bronkhorst flow meters. A set of flow meters with different full-scale ranges was used to reduce the uncertainties of measured flow rates to below 2% of the measured value. The equivalence ratios derived from the measured fuel and air flows have an uncertainty of ∼3%. Additionally, the equivalence ratios were derived independently

Received: September 10, 2019
Revised: October 22, 2019
Published: October 22, 2019

 © 2019 American Chemical Society

DOI: 10.1021/acs.energyfuels.9b03097
Energy Fuels 2019, 33, 11976−11984

from the concentration of oxygen (O_2) in the unburned gas/air mixture measured by a Maihak S 710 extractive gas analyzer, which improved the accuracy in φ (to ~1%). Both methods of determining φ gave the same values to within 3%. The temperature of the fuel/air mixtures was taken as 295 K. The uncertainties in measured equivalence ratios and exit velocities result in an uncertainty in setting the flame temperature of less than 20 K (see below). Due to the high pressure drop in the burner and low vapor pressure of DME (~4.4 bar) at room temperature, the highest exit velocity of the unburned DME/air mixture in the present setup is limited to 35 cm/s, which is lower than the free-flame burning velocity at φ = 1.0 (~44 cm/s) reported in other studies.[13−15] As a result, it was impossible to reach adiabatic conditions in DME flames with free-burning velocities higher than 35 cm/s. Although this limitation has few consequences for the results described below (which rely on the variations in flame temperature with exit velocity), it does limit the assessment of the uncertainty of the Raman measurements at higher temperatures. For this purpose, we use mixtures of methane (with a purity of 99.995%) and air at room temperature, for which 1D stabilized and free-burning flames can be obtained with equivalence ratios between 0.7 and 1.3, showing enough variation in absolute temperature for the assessment.

2.2. Temperature Measurements. The Raman setup used for temperature measurements in this study is similar to that described elsewhere[16] and utilized an Nd:YLF laser operating at a frequency of 5 kHz and producing averaged power of 30 W. The laser radiation was focused on the flame axial position at different heights above the burner (HAB), and the scattered signal was collected at 90°, dispersed by a spectrometer, and measured by a CCD camera. The exposure time for the signal acquisition by the CCD camera in the experiment was set at 2 min. Further extension of exposure time did not improve the quality of the Raman spectra significantly. The temperature was derived by fitting the measured Raman spectrum from nitrogen (N_2). A typical N_2 Raman spectrum in the DME/air flame at φ = 1.2, v = 25 cm/s, and HAB = 1.0 cm is shown in Figure 1. The fitting procedure

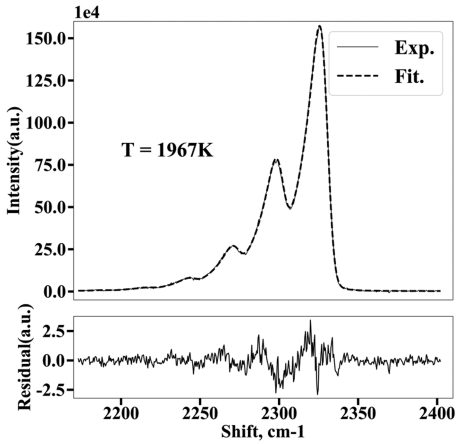

Figure 1. Measured and fitted N_2 Raman spectrum in DME/air flame at φ = 1.2, v = 25 cm/s, and HAB = 1 cm.

for this flame yields T = 1967 K. Vertical temperature profiles were measured by moving the burner first down ~2 cm from the initial position at HAB = 2 mm and then back with steps 2 mm, thus providing two profiles for the same experimental conditions. The differences in the derived temperatures were less than 20 K, indicating the short-term reproducibility (regarding flame conditions and positioning) of our measurements. The day-to-day reproducibility was also generally better than 20 K. Since the reproducibility of the temperature measurements was better than the estimated accuracy (~30 K, see below), the error bars in the temperature plots are ±30 K.

In addition to the visual control, the flatness of the flames was verified by measuring the horizontal temperature profiles at all exit velocities. A typical horizontal profile at a height of 1 cm for the stoichiometric flame with an exit velocity of 30 cm/s is shown in Figure 2. As can be seen, the temperature profile is flat with

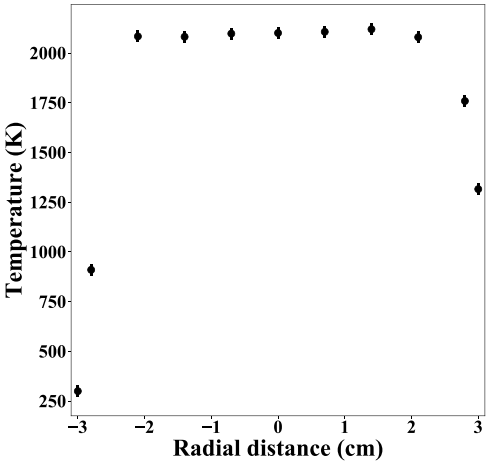

Figure 2. Radial temperature profile in methane/air flame at φ = 1.0, v = 30 cm/s, and HAB = 1 cm.

differences not exceeding 30 K at a radial distance less than 2 cm from the burner axis. The measured temperature horizontal profiles remain flat up to the heights of 2 cm even when exit velocity exceeds the free-burning velocity, and the 'hill' structure is observed visually instead of the flat flame front.

2.3. Modeling. The conservation equations for 1D flames were solved using the Cantera package.[17] The 'Mixture averaged' model[18] was used for the calculation of transport properties. In the calculations, the computation domain was set to 10 cm. The final solution was obtained with a grid of ~140 points. Further increase in the number of grid points resulted in temperature changes less than 10 K. The calculations were performed for both burner-stabilized and free flames. As a rule, the calculations did not converge in the burner-stabilized flames with exit velocities in the range higher than 80% of the free-burning velocity. For this velocity range, the calculated temperatures shown in the plots below are linearly interpolated. In the Cantera suite, the radiative heat losses are taken into account using the gray-gas approximation in the optically thin limit,[19] where CO_2 and H_2O are assumed as the only radiating species. Planck mean coefficients of CO_2 and H_2O are calculated using polynomials from refs 20 and 21.

2.4. Chemical Mechanisms. For the assessment of the temperature determination, methane/air flames were simulated using the GRI-Mech 3.0 mechanism, which contains 53 species and 325 elementary chemical reactions.[22]

For DME, three widely used chemical mechanisms were evaluated in this paper. Zhao model: The mechanism developed by Zhao et al.,[23] based on the studies of the unimolecular decomposition reaction of DME in a flow reactor at a temperature of 980 K and pressure of 10 atm, contains 55 species and 290 reactions. Below, we refer to this mechanism as the Zhao model. The free-flame burning velocities (S_L) of DME/air flames calculated using this model for equivalence ratios from 0.6 to 2.0 are shown in Figure 3. The mechanism proposed by Liu et al.[24] (the Liu model), obtained by adopting the hydrogen subset from ref 25 and updating the reaction rate constants of the Zhao model, includes 55 species and 295 reactions. The free-flame burning velocities calculated by the Liu model are also shown in Figure 3. As can be seen, the difference of predictions between these two models is marginal at lean (φ < 1.1) and rich (φ > 1.7) conditions, while the Liu model predicts higher S_L than the Zhao model at 1.1 < φ < 1.7. Finally, the mechanism developed by Burke et al.[26] ("NUIG Mech_56.54"), based on the studies of the ignition delay time of DME, methane, and their mixtures covering a range of conditions relevant to gas turbine environments. This model is more complex than the Zhao and Liu models and contains 113 species and

DOI: 10.1021/acs.energyfuels.9b03097
Energy Fuels 2019, 33, 11976−11984

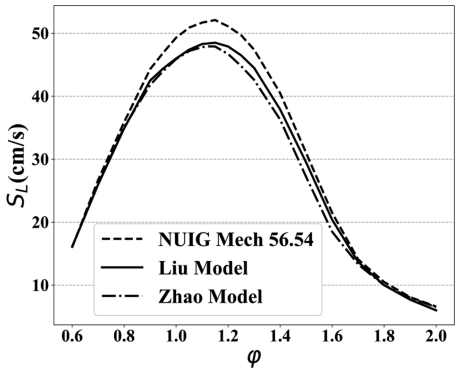

Figure 3. Calculated free-flame burning velocities of DME/air flames at a temperature of 295 K and a pressure of 1 atm.

710 reactions. Comparing with the Zhao and Liu models, NUIG Mech_56.54 predicts highest S_L at φ in the range from 0.8 to 1.7, while at leaner (φ < 0.8) and richer (φ > 1.7) conditions, the predicted S_L from all three models are indistinguishable as shown in Figure 3.

3. RESULTS AND DISCUSSION

3.1. Temperature Measurements in Methane/Air Flames. The accuracy of temperature measurements is assessed here by comparing the measured and calculated temperatures in "free-burning" flames, i.e., flames without heat transfer to the burner. The temperature of these flames can be calculated using thermodynamics, which would obviate uncertainties related to the impact of chemical kinetics. To achieve these conditions, the exit velocities of the unburned gas/air mixtures at a fixed equivalence ratio are progressively increased to the point at which the flame temperature is independent of exit velocity. As mentioned above, while the equilibrium temperatures for adiabatic DME/air flames are readily calculated, the free-burning exit velocity could not be reached for these flames under all conditions, and methane/air flames were used for this purpose. Figure 4 shows temperature profiles measured at φ = 1.0 and v = 10, 20, and 30 cm/s. As expected, the measured flame temperature increases with the exit velocity of the unburned mixture, from ~1700 K at v = 10 cm/s up to ~2050 K at v = 30 cm/s, indicating decreasing upstream heat losses to the burner surface. At the three exit velocities, the measured temperatures increase to a maximum and then begin to decrease toward the end of the measured domain, the decrease varying with exit velocity. The temperature profiles calculated using GRI-Mech 3.0 without radiative heat loss from the hot gases, as shown in Figure 4, display the usual increase in temperature from the slow approach to equilibrium caused by radical recombination in the post-flame gases, substantially overpredicting the (measured) temperature. Repeating the calculations while incorporating radiative heat loss improves the agreement with the measured profiles significantly, with a slight overestimate of the heat loss in the measurements for v = 10 cm/s at HAB > 1 cm. Very good agreement between the computed profiles with radiative heat losses and the measurements was also observed for other equivalence ratios and exit velocities, implying the necessity of including this heat loss mechanism in the analysis.

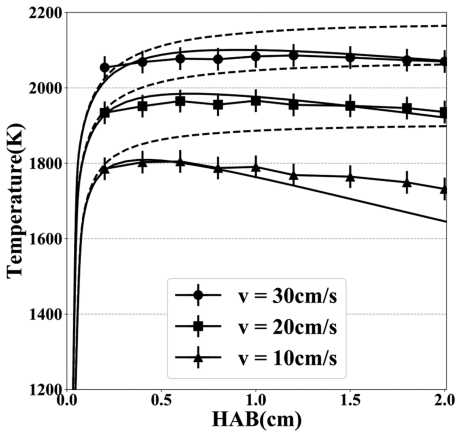

Figure 4. Axial temperature profiles in methane/air flames at φ = 1.0. Symbols: measurements in flames at exit velocities 30 cm/s (circles), 20 cm/s (squares), and 10 cm/s (triangles). Lines: calculations using GRI-Mech 3.0 with (solid) and without (dashed) radiative heat losses.

The impact of radiative losses on the measured temperature was further analyzed by measuring temperatures at a fixed axial distance (HAB = 1 cm) in stoichiometric methane/air flames while progressively increasing the exit velocity. The results of these measurements are shown in Figure 5. As can be seen, the measured temperature increases with increasing exit velocities up to ~38 cm/s. Above this velocity, close to the free-burning velocity for stoichiometric methane/air flames,[27,28] the measured temperature remains constant, indicating no heat transfer from the flame to the burner. While one would expect the measured flame temperature under these conditions to be the adiabatic stoichiometric value (~2225 K), the maximum measured temperature is ~2150 K. At HAB = 1 cm in a stoichiometric methane/air flame, the observation of a lower temperature can be ascribed to radiative losses and to being upstream of the point at which equilibrium is reached downstream of the burner. The flame temperatures were calculated with and without radiative heat losses as shown in Figure 5. The calculations without radiative heat losses overpredict the flame temperature ~60 K at v < 38 cm/s, while the calculations with radiative heat losses predict the flame temperature very well up to v = 38 cm/s. We examine this agreement further by varying the equivalence ratio and

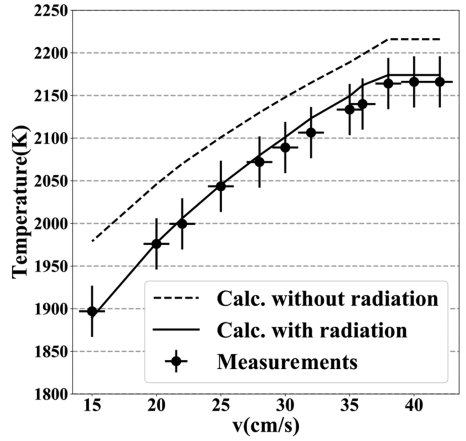

Figure 5. Measured (circles) and calculated temperatures with (solid line) and without (dashed line) radiative heat losses at HAB = 1 cm as a function of exit velocity in stoichiometric methane/air flames.

DOI: 10.1021/acs.energyfuels.9b03097
Energy Fuels 2019, 33, 11976−11984

comparing the measurements for the free-flame temperatures with the computations with and without radiation.

Similar measurements were performed at different equivalence ratios. The results of these measurements are presented in Figure 6, where the temperatures of free flames at HAB = 1 cm are shown. As can be seen, at all equivalence ratios, the measured flame temperatures are lower than adiabatic ones. In rich flames, the difference is ~40 K, at the stoichiometric flame, it is ~60 K and decreases to ~30 K in lean flames. The fact that the flame temperature measured by spontaneous Raman scattering is systematically lower than adiabatic was also observed previously.[29] As discussed above, we attribute this discrepancy to radiative heat losses, which can be substantial in high temperature flames.[30−32] To test this assumption, we performed calculations of 1D flames taking radiative heat losses into consideration. As can be seen in Figure 6, the calculations and measurements agree very well if the radiative heat losses are accounted for.

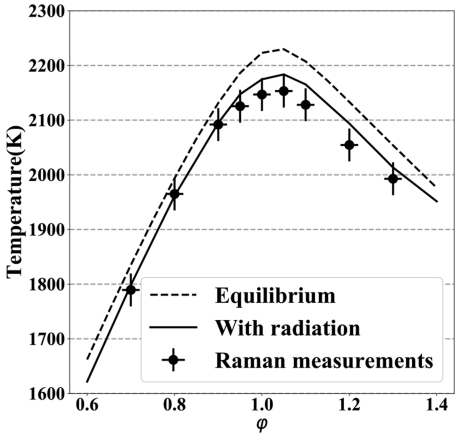

Figure 6. Methane/air flame temperature as a function of equivalence ratio at HAB = 1 cm. Measurements (circles) and calculations with (solid line) and without (dashed line) radiative heat losses.

Comparing the measured and calculated temperatures in free-burning flames, we estimate the accuracy of the Raman temperature measurements as 30 K. Therefore, in our analysis of the performance of the mechanisms below, we will only consider the disagreement between the measurements and calculations as significant if it exceeds 30 K. As mentioned above, this uncertainty is used in the figures showing temperature measurements.

3.2. Temperature Measurements in DME/Air Flames.

A typical vertical temperature profile in the DME/air flame at φ = 1.0 and v = 25 cm/s is shown in Figure 7, as well as the temperatures calculated using the Liu model with and without radiative heat losses. Calculations with other mechanisms yielded similar results and are not shown in Figure 7 to avoid clutter. As seen for the methane/air results presented above, the calculations without radiation overpredict the measured temperatures, while the inclusion of radiation brings the computed and measured temperature profiles to an agreement within the measurement uncertainty. Hence, we will use only the calculations with radiative heat loss for comparison with the measured temperatures in the discussion below.

The measured and calculated DME flame temperatures as a function of exit velocities at fixed HAB = 1 cm are shown in Figure 8, for equivalence ratios φ = 0.6, 0.8, 1.0, 1.4, 1.7, and 2.0. To view the full range of temperature variation and still amplify the differences observed, the axes for the different equivalence ratios are plotted on different scales; but for all data, the error bars of the measured flame temperature and exit velocity were set at 30 K and 1 cm/s, respectively, in all graphs in Figure 8. The highest computed exit velocities shown in the figures are those calculated free-flame burning velocities at the specified equivalence ratio shown in Figure 3. Experimentally, we take the free-flame burning velocity either as the exit velocity above which the measured flame temperature remains constant, as in Figure 5, or the exit velocity at which the measured flame temperature reaches the calculated free-flame temperature.

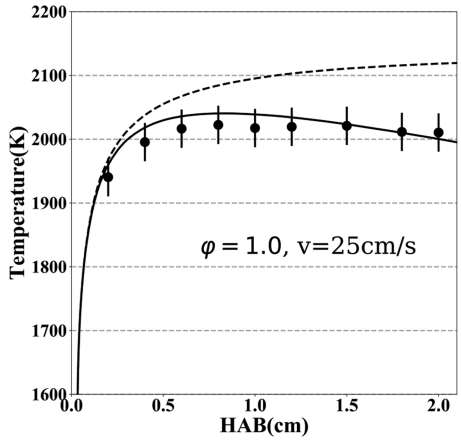

Figure 7. Axial temperature profiles in DME/air flames at φ = 1.0, v = 25 cm/s. Circles: measurements in flames, lines: calculations using the Liu model with (solid) and without (dashed) radiation.

At the lowest equivalence ratio φ = 0.6 (Figure 8a), stable flames could be obtained only in the range of exit velocities from 10 to 14 cm/s and the variations in flame temperature are only ~80 K in this range. While all three mechanisms predict temperatures within 20 K of each other, they underpredict the measurements by 30 K or more, i.e., larger than estimated accuracy of the temperature measurements as discussed above. Provided that the sensitivity of temperature to the rate of individual reactions does not change sign upon varying the exit velocity. For burner-stabilized flames, we recall that if the free-flame burning velocity is too high, then, at a given exit velocity ($v < S_L$) more heat must be transferred to the burner to reduce the actual burning velocity to the exit velocity. Accordingly, the observation that the computations consistently underpredict the flame temperature suggests a free-flame burning velocity that is too high. We remark that we could not make a stable flat flame at an exit velocity of ~16 cm/s, which is the predicted free-burning velocity for all three mechanisms, but we also observe that at the highest exit velocity attainable (~14 cm/s), the measured temperature has already reached that predicted for the free flame (~1700 K) at φ = 0.6. Thus, our measurements indicate that the free-burning velocity of DME/air flames at φ = 0.6 is roughly 14 cm/s. Most free-flame burning velocity measurements for DME/air flames were usually obtained in the range of φ = 0.7−1.9.[9,33−35] However, to our knowledge, the only measurement of the free-burning velocity at φ = 0.6 was performed by Wang et al.[2] and reported to be slightly less than that reported here, ~12 cm/s. The results shown in Figure 8a show temperature at 12 cm/s that is significantly lower than that at 14 cm/s, indicating that the value reported by Wang et al.[2] is too low. Being able to

DOI: 10.1021/acs.energyfuels.9b03097
Energy Fuels 2019, 33, 11976−11984

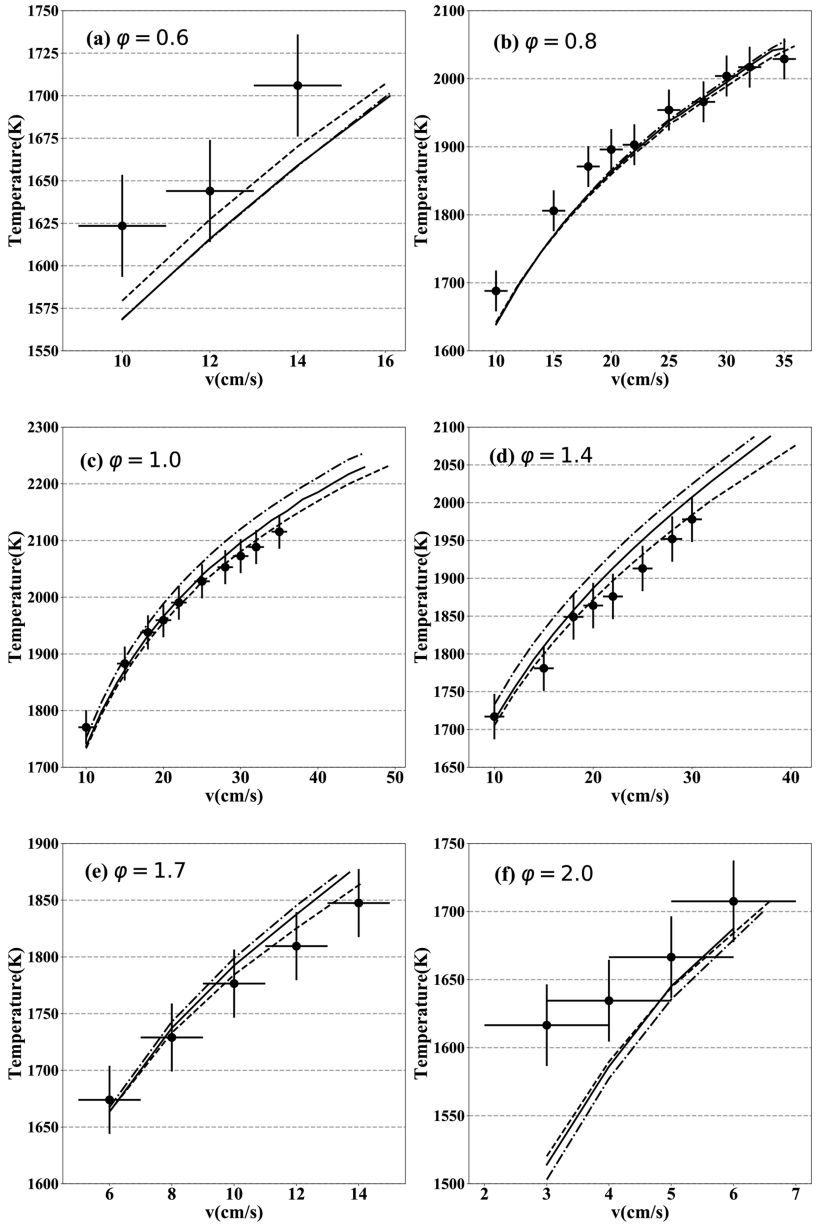

Figure 8. Measured (circles) and calculated (solid line—Liu model, dashed line—"NUIG Mech 56.54", dashed dot line—Zhao model) temperatures in DME/air flames at φ = 0.6 (a), φ = 0.8 (b), φ = 1.0 (c), φ = 1.4 (d), φ = 1.7 (e), and φ = 2.0 (f) as a function of exit velocity at HAB = 1 cm.

indicate whether a predicted (or measured) value is too high or too low is a substantial advantage of examining the behavior of burner-stabilized flames.

The differences among the calculated temperatures from all three mechanisms are even less at φ = 0.8 (Figure 8b). At this equivalence ratio, all three mechanisms slightly underestimate the measured flame temperatures ($\lesssim$30 K) in the range of v = 10−20 cm/s, which is consistent with the underestimation of flame temperature observed at φ = 0.6; the agreement between measurements and calculations is significantly improved at exit velocities above 20 cm/s (temperature above 1900 K).

In stoichiometric (Figure 8c) and rich (φ = 1.4, Figure 8d) flames, the differences among the temperatures predicted by the three mechanisms become more noticeable. The Zhao model always predicts the highest temperatures, while NUIG Mech_56.54 predicts the lowest temperature, ∼50 K lower than the Zhao model. The predictions of the Liu model lie between the other two mechanisms. This observation is consistent with the differences in the free-flame burning velocities shown in Figure 3: at φ = 1.0, 46, 45.9, and 49.3 cm/s are predicted by the Zhao, Liu, and NUIG Mech_56.54 models, respectively, and 36.3, 37.9, and 40.5 cm/s at φ = 1.4. At φ = 1.0, all three models represent the experimental results well at v < 20 cm/s, but diverge at a higher exit velocity; at v > 20 cm/s, the Liu model is still within the experimental uncertainty of the temperature measurements, while NUIG Mech 56.54 is in very good agreement with the experiments and the predictions of the Zhao model are outside the measurement uncertainty, by nearly 50 K. Similar trends are observed at φ = 1.4 over the entire range of exit velocity studied. These results suggest that the free-flame burning velocities are closer to 49 and 40 cm/s for φ = 1.0 and 1.4, respectively.

DOI: 10.1021/acs.energyfuels.9b03097
Energy Fuels 2019, 33, 11976−11984

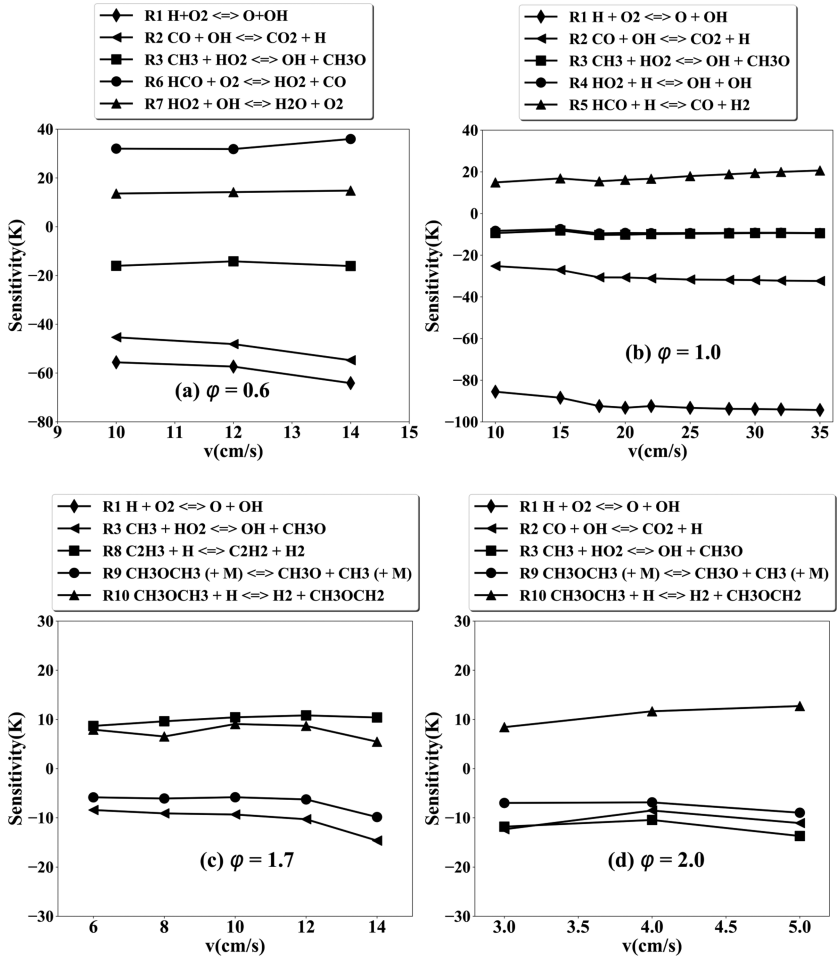

Figure 9. Sensitivity coefficient for temperatures at HAB = 1 cm as a function of exit velocity in DME flame, φ = 0.6 (a), φ = 1.0 (b), φ = 1.7 (c), and φ = 2.0 (d).

For φ = 1.7 in Figure 8e, the DME flame can only be stabilized in the range of exit velocities 6−14 cm/s. All three mechanisms predict the measured temperatures within 30 K; the three mechanisms predict free-flame burning velocities within 13.5 ± 0.5 cm/s.

In the richest flame, φ = 2.0 in Figure 8f, the exit velocities were limited in the range of 3−6 cm/s. Allowing for the difficulty in stabilizing a fuel-rich flame at exit velocities below 5 cm/s, which we ascribe to buoyancy effects, we only remark that the three mechanisms tend to underestimate the flame temperature. To our knowledge, the free-burning velocity of the DME/air flame at φ = 2.0 has not been measured previously, but, based on the measured temperature, the results indicate a free-burning velocity ∼6 cm/s. Considering the ±1 cm/s uncertainty of the measurements, we consider the computed free-flame burning velocities in the range of 6−6.6 cm/s to be in good agreement with the measurements shown.

Summarizing, the overall performance of the chemical mechanisms in the prediction of flame temperatures as a function of equivalence ratio is good in the region φ = 0.8−1.7, with more deviation at 0.6 and 2.0. Below, we explore the possibility of using the method to improve the model predictions.

3.3. Sensitivity Analysis of Flame Temperature to Variation of Rates of Chemical Reactions. To clarify the performance of the chemical mechanisms in the prediction of the measured flame temperatures, we perform a sensitivity analysis. The calculations were performed using the Liu model; its performance is similar to NUIG Mech_56.54, but its smaller size facilitates the analysis. For this purpose, we vary the pre-exponential factor of the Arrhenius equation for the *i*th reaction A_i by 50% and calculate the sensitivity coefficients by

$$S_i = 2^*(T(x, 1.5A_i) - T(x, A_i))$$

where $T(x, 1.5A_i)$ and $T(x, A_i)$ are temperatures calculated at distance x with $1.5A_i$ and A_i, respectively. In this formulation, the sensitivity coefficient is the temperature change when increasing A_i by 50%, assuming a linear dependence of temperature upon the rates of chemical reactions.

The sensitivity analysis was performed for flames at equivalence ratios φ = 0.6, 1.0, 1.7, and 2.0 for the exit velocities used in the experiments. The results of the sensitivity analysis at HAB = 1.0 cm are presented in Figure 9a−d, only the five most important reactions are shown in the plot for each equivalence ratio. We first observe that, in contrast to the results for hydrogen/air flames,[11] the impact of most sensitive reactions is slightly dependent on exit velocity (differences less than 10 K). Consequently, the variation of the rates of these reactions will do little to affect the curvature of the plots of flame temperature vs. exit velocity.

For the stoichiometric DME/air flame (Figure 9b), the chain branching reaction

$$H + O_2 \Leftrightarrow O + OH \qquad (R1)$$

DOI: 10.1021/acs.energyfuels.9b03097
Energy Fuels 2019, 33, 11976−11984

has the highest sensitivity $S_{R1} \approx -90$ K, while the reaction of CO oxidation

$$CO + OH \Leftrightarrow H + CO_2 \quad (R2)$$

takes the second place with $S_{R2} \approx -30$ K. Reactions

$$CH_3 + HO_2 \Leftrightarrow OH + CH_3O \quad (R3)$$

and

$$HO_2 + H \Leftrightarrow OH + OH \quad (R4)$$

have close negative sensitivity coefficients (roughly −20 K), while only reaction

$$HCO + H \Leftrightarrow CO + H_2 \quad (R5)$$

shows a positive influence, ∼20 K, on the flame temperature. Recalling the discussion above, reactions that increase the free-flame burning velocity will reduce the temperature of the burner-stabilized flame. Of course, these five reactions are also the most sensitive reactions for the free-burning velocity in stoichiometric methane/air flame.[34,36−38]

At $\varphi = 0.6$, reactions R1−RRR3 remain the most important reactions, with sensitivity coefficients $S_{R1} \approx -60$ K, $S_{R2} \approx -40$ K, and $S_{R3} \approx -20$ K, respectively, while reactions R4 and RRR5 are replaced by

$$HCO + O_2 \Leftrightarrow HO_2 + CO \quad (R6)$$

with the sensitivity coefficient $S_{R6} \approx 30$ K and

$$HO_2 + OH \Leftrightarrow HO_2 + O_2 \quad (R7)$$

with the sensitivity coefficient $S_{R7} \approx 15$ K. The most sensitive reactions (Figure 9a) for DME flame at $\varphi = 0.6$ are also important for methane/air flames.[39] To improve the agreement between the measured and computed temperatures, the latter must be increased. That is, the free-flame burning velocity must be reduced. This implies decreasing the rate of R1−R3 or increasing the rates of R6/R7. However, given the importance of these reactions in the burning velocity of methane, the impact of any changes in these rates on the predictions for methane would have to be assessed simultaneously. As such, we refrain from doing so here.

At $\varphi = 1.7$, reaction R1 (not shown in Figure 9c) and R3 still show the highest sensitivity, with coefficients $S_{R1} \approx -100$ K and $S_{R3} \approx -10$ K, respectively. Moreover, three new reactions appear in the list of most sensitive reactions: the reaction between vinyl radical and hydrogen

$$C_2H_3 + H \Leftrightarrow C_2H_2 + H_2 \quad (R8)$$

the decomposition reaction of DME

$$CH_3OCH_3(+M) \Leftrightarrow CH_3O + CH_3(+M) \quad (R9)$$

and H atom abstraction from DME

$$CH_3OCH_3 + H \Leftrightarrow H_2 + CH_3OCH_2 \quad (R10)$$

At the richest conditions, $\varphi = 2.0$, reaction R1 still has the largest negative sensitivity ($S_{R1} \approx -90$ K, not shown in Figure 9d) and reaction R10 shows the largest positive sensitivity $S_{R10} \approx 10$ K. Three other reactions R2, R3, and R9 have S_i of roughly −10 K. At $\varphi = 2.0$, considering only the two highest points, as mentioned above, the calculated temperatures are within the vertical and horizontal error bars. Although the predictions for $\varphi = 1.7$ are also reasonably close to the measurements, we use this equivalence ratio to examine the potential improved agreement by varying two of the rate constants. Since both R9 and R10 are sensitive reactions at this equivalence ratio and only consider DME, we choose these reactions as an example. Since the predicted temperatures must decrease to improve the agreement of this mechanism with the experimental temperatures, the rate of R9 should be increased and/or R10 should be decreased. Figure 10 shows the results

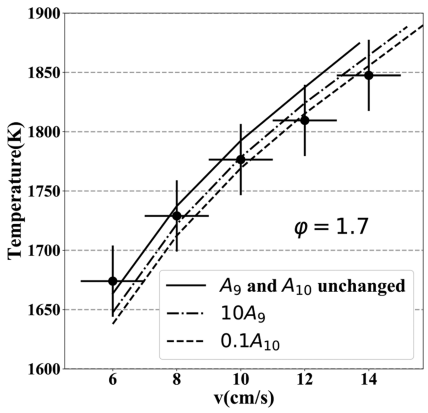

Figure 10. Measured (circles) and calculated temperatures as a function of exit velocity at HAB = 1 cm, $\varphi = 1.7$. Solid line: with reaction rates unchanged, dashed dot line: the rate of reaction R9 increased by a factor 10, dashed line: the rate of reaction R10 decreased by a factor 10.

of increasing R9 by a factor of 10 and by reducing R10 by the same factor. This is outside the range of uncertainty of these reactions.[40,41] Both of these changes bring the predictions of the Liu model at higher exit velocity closer to the experiments while maintaining the agreement at lower velocities. We note that the change in R9 increases the free-flame burning velocity to 15.2 cm/s, while the decrease in the rate of R10 increases the burning velocity to 15.7 cm/s.

4. CONCLUSIONS

The temperatures of burner-stabilized premixed 1D DME/air flames at various exit velocities were measured using spontaneous Raman scattering to evaluate DME chemical mechanisms for predicting burning velocity. The method allows testing mechanisms under nonadiabatic conditions at (strongly) reduced temperatures. Comparison of measured and calculated flame temperatures in free-burning CH4/air flames show that radiative heat losses must be incorporated when evaluating the predictions of chemical mechanisms. In addition, we observe that the comparison of the measured and computed temperatures permits conclusions regarding whether a computed free-flame burning velocity is too high or too low.

Regarding the performance of the three mechanisms of DME oxidation studied:

(1) The calculations using NUIG Mech_56.54 and the Liu model generally predict the results within the experimental uncertainty for flames in the range $\varphi = 0.8-1.7$. The Zhao model predicts the highest temperature among all of the three mechanisms and fails to capture the temperatures in flames with high exit velocities at $\varphi = 1.0$ and 1.4. All of the three mechanisms underpredict the temperatures more than 30 K at $\varphi = 0.6$ and are at the limits of the experimental uncertainty at the highest exit velocities at $\varphi = 2.0$. The apparent leveling off of the measured flame temperature at 3 and 4 cm/s is herein

DOI: 10.1021/acs.energyfuels.9b03097
Energy Fuels 2019, 33, 11976−11984

attributed to buoyancy effects, excluding them from use in further analysis. The measured temperature at the highest exit velocity (6 cm/s) at φ = 2.0 indicates that the predicted range of the free-flame burning velocity (6−6.6 cm/s) is close to the true value.

(2) The underprediction of the measured temperatures at φ = 0.6 suggests that the computed free-flame burning velocity of 16 cm/s for this equivalence ratio is too high; the measured temperatures indicate a burning velocity closer to 14 cm/s.

(3) The sensitivity analysis of the important reactions for DME in the Liu model (as an example) at the equivalence ratios studied shows that, in contrast to hydrogen/air flames, the sensitivity of the predicted temperatures to the reaction rate is essentially insensitive to the exit velocity. Thus, the variation of the reaction rates will not affect the curvature of the T vs. v plot. Reactions involving DME only appeared in the five most sensitive reactions in rich DME flames, φ = 1.7 and 2.0. Increasing the rates of the decomposition reaction R9 or decreasing the reaction describing H abstraction from DME (RRR10) by a factor of ten (or less) improved the agreement with the measurements, implying an increase in free-flame burning velocity by 2 cm/s or less.

AUTHOR INFORMATION

Corresponding Author

*E-mail: a.v.mokhov@rug.nl.

ORCID

Anatoli Mokhov: 0000-0002-5791-7528

Notes

The authors declare no competing financial interest.

ACKNOWLEDGMENTS

L.D. thanks the China Scholarship Council (CSC) for financial support.

ABBREVIATIONS

DME = dimethyl ether
φ = equivalence ratio
v = exit velocity of unburned mixture
1D = one dimensional
HAB = height above burner
S_L = free-burning velocity of laminar flame
A_i = pre-exponential factor of the Arrhenius equation for the ith reaction

REFERENCES

(1) Kim, M. Y.; Yoon, S. H.; Ryu, B. W.; Lee, C. S. Combustion and Emission Characteristics of DME as an Alternative Fuel for Compression Ignition Engines with a High Pressure Injection System. *Fuel* **2008**, *87*, 2779−2786.

(2) Wang, Y. L.; Holley, A. T.; Ji, C.; Egolfopoulos, F. N.; Tsotsis, T. T.; Curran, H. J. Propagation and Extinction of Premixed Dimethyl-Ether/Air Flames. *Proc. Combust. Inst.* **2009**, *32 I*, 1035−1042.

(3) Park, S. H.; Lee, C. S. Applicability of Dimethyl Ether (DME) in a Compression Ignition Engine as an Alternative Fuel. *Energy Convers. Manag.* **2014**, *86*, 848−863.

(4) Zhao, Y.; Wang, Y.; Li, D.; Lei, X.; Liu, S. Combustion and Emission Characteristics of a DME (Dimethyl Ether)-Diesel Dual Fuel Premixed Charge Compression Ignition Engine with EGR (Exhaust Gas Recirculation). *Energy* **2014**, *72*, 608−617.

(5) Wang, Q.; Dai, L.; Wu, K.; Bai, J.; He, Z. Study on the Combustion Process and Work Capacity of a Micro Free-Piston Engine. *J. Mech. Sci. Technol.* **2015**, *29*, 4993−5000.

(6) Hermanns, R. T. E.; Konnov, A. A.; Bastiaans, R. J. M.; de Goey, L. P. H.; Lucka, K.; Köhne, H. Effects of Temperature and Composition on the Laminar Burning Velocity of CH4 + H2 + O2 + N2 Flames. *Fuel* **2010**, *89*, 114−121.

(7) Zhao, Z.; Kazakov, A.; Dryer, F. L. Measurements of Dimethyl Ether/Air Mixture Burning Velocities by Using Particle Image Velocimetry. *Combust. Flame* **2004**, *139*, 52−60.

(8) Daly, C. A.; Simmie, J. M.; Würmel, J.; DjebaÏli, N.; Paillard, C. Burning Velocities of Dimethyl Ether and Air. *Combust. Flame* **2001**, *125*, 1329−1340.

(9) John, R.; Kishore, V. R.; Akram, M.; Yoon, Y.; Kumar, S. Burning Velocities of DME (Dimethyl Ether) -Air Premixed Flames at Elevated Temperatures. *Energy* **2017**, *126*, 34−41.

(10) Botha, J. P.; Spalding, D. The Laminar Flame Speed of Propane/Air Mixtures with Heat Extraction from the Flame. *Proc. R. Soc. London, Ser. A* **1954**, *225*, 71−96.

(11) Sepman, A. V.; Mokhov, A. V.; Levinsky, H. B. Extending the Predictions of Chemical Mechanisms for Hydrogen Combustion: Comparison of Predicted and Measured Flame Temperatures in Burner-Stabilized, 1D Flames. *Int. J. Hydrogen Energy* **2011**, *36*, 9298−9303.

(12) Kaskan, W. E. The Dependence of Flame Temperature on Mass Burning Velocity. *Proc. Combust. Inst.* **1957**, *6*, 134−143.

(13) Qin, X.; Ju, Y. Measurements of Burning Velocities of Dimethyl Ether and Air Premixed Flames at Elevated Pressures. *Proc. Combust. Inst.* **2005**, *30*, 233−240.

(14) Huang, Z.; Wang, Q.; Yu, J.; Zhang, Y.; Zeng, K.; Miao, H.; Jiang, D. Measurement of Laminar Burning Velocity of Dimethyl Ether-Air Premixed Mixtures. *Fuel* **2007**, *86*, 2360−2366.

(15) Yu, H.; Hu, E.; Cheng, Y.; Zhang, X.; Huang, Z. Experimental and Numerical Study of Laminar Premixed Dimethyl Ether/Methane−Air Flame. *Fuel* **2014**, *136*, 37−45.

(16) Mokhov, A. V.; Levinsky, H. B.; van der Meij, C. E. Temperature Dependence of Laser-Induced Fluorescence of Nitric Oxide in Laminar Premixed Atmospheric-Pressure Flames. *Appl. Opt.* **1997**, *36*, 3233−3243.

(17) Goodwin, D. G.; Moffat, H. K.; Speth, R. L. *Cantera: An Object-Oriented Software Toolkit for Chemical Kinetics, Thermodynamics, and Transport Processes*, version 2.3.0, 2017.

(18) Kee, R. J.; Coltrin, M. E.; Glarborg, P. *Chemically Reacting Flow : Theory and Practice TT*; Wiley-Interscience: Hoboken, NJ, 2003.

(19) Liu, Y.; Rogg, B. Prediction of Radiative Heat Transfer in Laminar Flames. *Combust. Sci. Technol.* **1996**, *118*, 127−145.

(20) Sandia national lab TNF workshop. http://www.sandia.gov/TNF/radiation.html.

(21) Grosshandler, W. L. RADCAL: A Narrow-Band Model for Radiation Calculations in a Combustion. *Environment NIST Tech. Note*, 1993

(22) Smith, G. P., Golden, D. M., Frenklach, M., Moriarty, N. W., Eiteneer, B., Goldenberg, M., et al. http://combustion.berkeley.edu/gri-mech/.

(23) Zhao, Z.; Chaos, M.; Kazakov, A.; Dryer, F. L. Thermal Decomposition Reaction and a Comprehensive Kinetic Model of Dimethyl Ether. *Int. J. Chem. Kinet.* **2008**, *40*, 1−18.

(24) Liu, D.; Santner, J.; Togbé, C.; Felsmann, D.; Koppmann, J.; Lackner, A.; Yang, X.; Shen, X.; Ju, Y.; Kohse-Höinghaus, K. Flame Structure and Kinetic Studies of Carbon Dioxide-Diluted Dimethyl Ether Flames at Reduced and Elevated Pressures. *Combust. Flame* **2013**, *160*, 2654−2668.

(25) Burke, M. P.; Chaos, M.; Ju, Y.; Dryer, F. L.; Klippenstein, S. J. Comprehensive H 2/O 2 Kinetic Model for High-Pressure Combustion. *Int. J. Chem. Kinet.* **2012**, *44*, 444−474.

(26) Burke, U.; Somers, K. P.; O'Toole, P.; Zinner, C. M.; Marquet, N.; Bourque, G.; Petersen, E. L.; Metcalfe, W. K.; Serinyel, Z.; Curran, H. J. An Ignition Delay and Kinetic Modeling Study of Methane,

DOI: 10.1021/acs.energyfuels.9b03097
Energy Fuels 2019, 33, 11976−11984

Dimethyl Ether, and Their Mixtures at High Pressures. *Combust. Flame* **2015**, *162*, 315−330.
(27) Hassan, M. I.; Aung, K. T.; Faeth, G. M. Measured and Predicted Properties of Laminar Premixed Methane/Air Flames at Various Pressures. *Combust. Flame* **1998**, *115*, 539−550.
(28) de Goey, L. P. H.; van Maaren, A.; Quax, R. M. Stabilization of Adiabatic Premixed Laminar Flames on a Flat Flame Burner. *Combust. Sci. Technol.* **1993**, *92*, 201−207.
(29) Sepman, A. V.; Toro, V. V.; Mokhov, A. V.; Levinsky, H. B. Determination of Temperature and Concentrations of Main Components in Flames by Fitting Measured Raman Spectra. *Appl. Phys. B* **2013**, *112*, 35−47.
(30) Guiberti, T. F.; Garnier, C.; Scouflaire, P.; Caudal, J.; Labegorre, B.; Schuller, T.; Darabiha, N. Experimental and Numerical Analysis of Non-Catalytic Partial Oxidation and Steam Reforming of CH4/O2/N2/H2O Mixtures Including the Impact of Radiative Heat Losses. *Int. J. Hydrogen Energy* **2016**, *41*, 8616−8626.
(31) Haider, S. *PAPER NO .: 274 Combustion and Radiation Modeling of Laminar Premixed Flames Using OpenFOAM : A Numerical Investigation of Radiative Heat Transfer in the RADIADE Project*, 27th CIMAC World Congr., 2013.
(32) Lamoureux, N.; Marschallek-Watroba, K.; Desgroux, P.; Pauwels, J. F.; Sylla, M. D.; Gasnot, L. Measurements and Modelling of Nitrogen Species in CH4/O2/N2flames Doped with NO, NH3, or NH3+NO. *Combust. Flame* **2017**, *176*, 48−59.
(33) Yu, H.; Hu, E.; Cheng, Y.; Yang, K.; Zhang, X.; Huang, Z. Effects of Hydrogen Addition on the Laminar Flame Speed and Markstein Length of Premixed Dimethyl Ether-Air Flames. *Energy Fuels* **2015**, *29*, 4567−4575.
(34) Ranzi, E.; Frassoldati, A.; Grana, R.; Cuoci, A.; Faravelli, T.; Kelley, A. P.; Law, C. K. Hierarchical and Comparative Kinetic Modeling of Laminar Flame Speeds of Hydrocarbon and Oxygenated Fuels. *Prog. Energy Combust. Sci.* **2012**, *38*, 468−501.
(35) De Vries, J.; Lowry, W. B.; Serinyel, Z.; Curran, H. J.; Petersen, E. L. Laminar Flame Speed Measurements of Dimethyl Ether in Air at Pressures up to 10 Atm C3 Mechanism Is Used Here. *Fuel* **2011**, *90*, 331−338.
(36) Warnatz, J. The Structure of Laminar Alkane-, Alkene-, and Acetylene Flames. *Symp. Combust.* **1981**, *18*, 369−384.
(37) Konnov, A. A. The Effect of Temperature on the Adiabatic Laminar Burning Velocities of CH4-Air and H2-Air Flames. *Fuel* **2010**, *89*, 2211−2216.
(38) Warnatz, J.; Maas, U.; Dibble, R. W. *Combustion*, 4th ed.; Springer-Verlag: Berlin Heidelberg, 2006.
(39) Metcalfe, W. K.; Burke, S. M. S. M.; Ahmed, S. S.; Curran, H. J. A Hierarchical and Comparative Kinetic Modeling Study of C1−C2 Hydrocarbon and Oxygenated Fuels. *Int. J. Chem. Kinet.* **2013**, *45*, 638−675.
(40) Sivaramakrishnan, R.; Michael, J. V.; Wagner, A. F.; Dawes, R.; Jasper, A. W.; Harding, L. B.; Georgievskii, Y.; Klippenstein, S. J. Roaming Radicals in the Thermal Decomposition of Dimethyl Ether: Experiment and Theory. *Combust. Flame* **2011**, *158*, 618−632.
(41) Tranter, R. S.; Lynch, P. T.; Yang, X. Dissociation of Dimethyl Ether at High Temperatures. *Proc. Combust. Inst.* **2013**, *34*, 591−598.

DOI: 10.1021/acs.energyfuels.9b03097
Energy Fuels 2019, 33, 11976−11984